

# Solving PDE's with FEniCS

## Adaptive meshes

### Chapter 16

### Introduction to Automated Modeling with FEniCS

by L. Ridgway Scott

We have seen different examples of localized singularities

- due to non-convex boundaries
- due to point loads

for the Laplace equation

$$\begin{aligned} -\Delta u &= f \text{ in } \Omega \\ u &= g \text{ on } \partial\Omega. \end{aligned} \tag{1}$$

Adaptive mesh refinement can approximate localized singularities more efficiently.

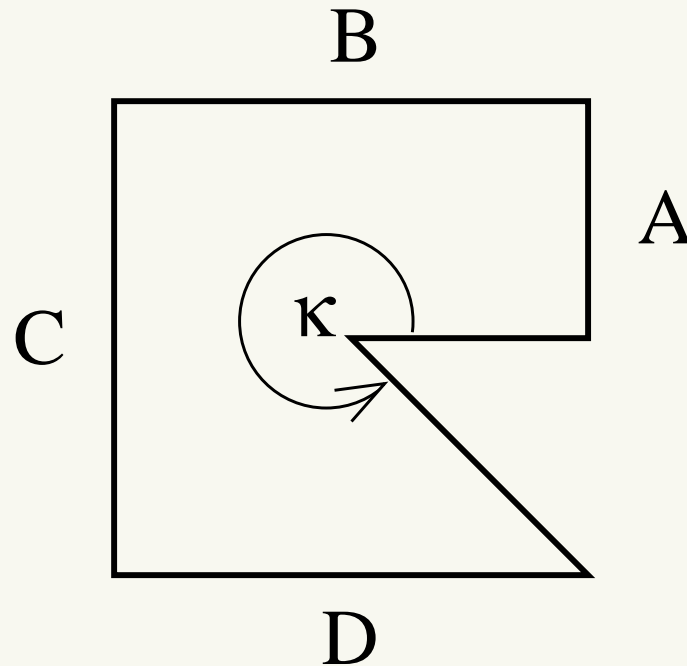


Figure 1: Re-entrant corner of angle  $\kappa$ .

Principle singularity for such a domain is of the form

$$u(r(\cos \theta, \sin \theta)) \approx r^{\pi/\kappa} \sin((\pi/\kappa)\theta). \quad (2)$$

When  $\kappa > \pi$  (nonconvex vertex),  $\nabla u$  is unbounded.

## Form of singularity

More precisely, for a re-entrant corner of angle  $\kappa$ ,

$$|\nabla^k u(r(\cos \theta, \sin \theta))| \approx r^{(\pi/\kappa)-k}$$

Here  $\nabla^k u$  denotes tensor of derivatives of  $u$  of order  $k$ .

Similarly, for a point load at  $r = 0$

$$|\nabla^k u(r(\cos \theta, \sin \theta))| \approx r^{2-d-k}$$

These singularities are of the form  $r^{\gamma-k}$  where  $\gamma \geq 0$  is fixed.

Now we consider appropriate meshes for approximating such functions.

## Mesh refinements for singularities

Suppose that, in general,

$$|\nabla^k u(\mathbf{r})| \approx C |\mathbf{r} - \mathbf{r}_0|^{-k+\gamma} \text{ for } \mathbf{r} \in \Omega, \quad (3)$$

where  $\nabla^k u$  denotes tensor of partial derivatives of order  $k$ , and  $|\mathbf{T}|$  denotes the Frobenius norm of a tensor  $\mathbf{T}$ .

For the L-shaped problem, we saw this holds for  $k = 1$  and  $\gamma = 2/3$ .

(3) holds for all  $k \geq 1$  and  $\gamma = \pi/\kappa$  for boundary vertices with angle  $\kappa$ .

For simplicity, we assume that  $\mathbf{r}_0 = 0$  from now on.

For a non-uniform mesh,

$$\begin{aligned}\|u - I_h u\|_{H^1(\Omega)}^2 &= \sum_e \|u - I_h u\|_{H^1(e)}^2 \\ &\leq C \sum_e \left( h_e^{m-1} \|u\|_{H^m(e)} \right)^2,\end{aligned}\tag{4}$$

where summation is over all of elements  $e$  of mesh and  $h_e = \text{size of } e$ .

Since we are assuming that the derivatives of the solution degrade in a radial fashion, let us also assume that the mesh is refined in a radial fashion.

## Optimal mesh refinements

For each element  $e$ , let  $\mathbf{r}_e$  denote its centroid.

Assume there is a monotonic mesh function  $\mu$  such that  $h_e \approx (1/n)\mu(|\mathbf{r}_e|)$ , where  $n$  is a mesh size parameter.

For example, we will consider  $\mu(r) = r^\beta$  for  $\beta > 0$ .

Let  $|e|$  denote the volume of an element  $e$ .

With such a mesh and under the assumption (3), the error expression (4) takes the form

$$\begin{aligned} & n^{2-2m} \sum_e \left( \mu(|\mathbf{r}_e|)^{m-1} |\mathbf{r}_e|^{-m+\gamma} \sqrt{|e|} \right)^2 \\ & \approx n^{2-2m} \int_{\Omega} \left( \mu(|\mathbf{r}|)^{m-1} |\mathbf{r}|^{-m+\gamma} \right)^2 d\mathbf{r}. \end{aligned} \tag{5}$$

## Optimal mesh conditions

Taking  $\mu(r) = r^\beta$ , the integrand in (5) simplifies to  $|\mathbf{r}|^p$  where  $p = 2(\beta(m - 1) - m + \gamma)$ .

Such an expression is integrable in  $d$  dimensions if and only if  $p > -d$ , that is, if

$$\beta > \frac{m - \gamma - d/2}{m - 1}.$$

If  $d = 2$  and  $m = 2$  (piecewise linears in 2 D), requirement is  $\beta > 1 - \gamma$ .

For the L-shaped domain, this means  $\beta > \frac{1}{3}$ .

## Optimal mesh conditions continued

For higher-order approximations, mesh conditions are different.

Other corners of the L-shaped domain can also require mesh refinement.

For these,  $\gamma = 2$ , and cubics ( $m = 4$ ) requires  $\beta > \frac{1}{3}$ .

In this case,  $\beta > 7/9$  is required at the re-entrant corner (for  $m = 4$ ).

When  $\gamma = \pi/\kappa$  is sufficiently large  
(comparable with  $m - d/2$ ), we can take  
 $\beta \approx 0$ , meaning a mesh of uniform size.

We have seen that refined meshes improve approximation substantially.

Such meshes are derived analytically based on a priori information about the singularities of the solution.

Possible to refine meshes automatically based on preliminary computations using techniques that estimate size of error for a given mesh.

Not at all obvious; requires explanation.

## Error indicators

One of the major advances of computational mathematics in the 20th century was the development of error indicators [4, Chapter 9].

Such indicators suggest where the computational error is largest and thus where the mesh should be refined.

This concept was pioneered by Ivo Babuška [2], primarily by focusing on the **residual error**.

Not at all obvious that the residual could indicate where the error is large, but it is now well understood.

The subject has developed significantly in the subsequent decades [1, 7, 9].

Many successful error estimators are based on the **residual**.

Consider the variational form

$$a_\alpha(v, w) = \int_{\Omega} \alpha(x) \nabla v(x) \cdot \nabla w(x) d\mathbf{x} \quad (6)$$

with  $\alpha$  piecewise smooth, but not necessarily continuous.

We will study the corresponding variational problem with Dirichlet boundary conditions on a polyhedral domain  $\Omega$  in the  $n$  dimensions, so that  $V = H_0^1(\Omega)$ .

## Model problem

For simplicity, take the right-hand side for the variational problem to be a piecewise smooth function,  $f$ .

As usual, let  $V_h$  be piecewise polynomials of degree less than  $k$  on a mesh  $T_h$ , and assume that the discontinuities of  $\alpha$  and  $f$  fall on mesh faces (edges in two dimensions) in  $T_h$ .

That is, both  $\alpha$  and  $f$  are smooth on each  $T \in T_h$ .

However, we will otherwise only assume that  $T_h$  is non-degenerate [4], since we will want to allow significant local mesh refinement.

## Mesh terminology

A family of meshes  $\{T_h\}$  is nondegenerate if there is a constant  $C < \infty$  such that  $\forall h$

$$\rho_{\max}(e) \leq C \rho_{\min}(e) \quad \forall e \in T_h \quad (7)$$

Here  $\rho_{\min}(e)$  (resp.,  $\rho_{\max}(e)$ ) is the radius of the largest ball contained in  $e$  (resp., smallest ball containing  $e$ ).

A mesh family is quasi-uniform if there is a constant  $C < \infty$  such that

$$h = \max \{ \rho_{\max}(e) : e \in T_h \} \leq C \min \{ \rho_{\min}(e) : e \in T_h \}$$

for all  $h$ .

## Degenerate meshes

Note that any quasi-uniform family of meshes is necessarily nondegenerate.

There are important classes of meshes that **are** degenerate.

- problems with a large aspect ratio
- problems where there is a discrepancy between the approximation needs in one direction versus others.

Significant work regarding error estimators in such an anisotropic context has been done

However, the subsequent material will be limited to the case of nondegenerate meshes.

## Residual definition

Let  $u$  satisfy the usual variational formulation  $a_\alpha(u, v) = (f, v)_{L^2(\Omega)}$  for all  $v \in V$ , and let  $u_h \in V_h$  be the standard Galerkin approximation.

The residual  $R_h \in V'$  is defined by

$$R_h(v) = a_\alpha(u - u_h, v) \quad \forall v \in V. \quad (8)$$

Note that, by definition,

$$R_h(v) = 0 \quad \forall v \in V_h, \quad (9)$$

assuming  $V_h \subset V$ .

Let  $\mathcal{A}$  denote the differential operator formally associated with the form (6), that is,  $\mathcal{A}v := -\nabla \cdot (\alpha \nabla v)$ .

## Residual computation

The residual can be computed by  $R_h(v) =$

$$\begin{aligned} & \sum_T \int_T (f + \nabla \cdot (\alpha \nabla u_h)) v \, dx + \sum_e \int_e [\alpha \mathbf{n}_e \cdot \nabla u_h]_{\mathbf{n}_e} v \, ds = \\ & \sum_T \int_T (f - \mathcal{A}u_h) v \, dx + \sum_e \int_e [\alpha \mathbf{n}_e \cdot \nabla u_h]_{\mathbf{n}_e} v \, ds \quad \forall v \in V, \end{aligned}$$

where  $\mathbf{n}_e$  denotes a unit normal to  $e$  and  $[\phi]_{\mathbf{n}}$  denotes the jump in  $\phi$  across the face normal to  $\mathbf{n}$ :

$$[\phi]_{\mathbf{n}}(x) := \lim_{\epsilon \rightarrow 0} \phi(x + \epsilon \mathbf{n}) - \phi(x - \epsilon \mathbf{n}).$$

so expression above is independent of choice of normal  $\mathbf{n}$  on each face.

## Jump terms

There are two parts to the residual.

One is the integrable function  $R_A$  defined on each element  $T$  by

$$R_A|_T := (f + \nabla \cdot (\alpha \nabla u_h))|_T = (f - \mathcal{A}u_h)|_T, \quad (10)$$

and the other is the “jump” term

$$R_J(v) := \sum_e \int_e [\alpha \mathbf{n}_e \cdot \nabla u_h]_{\mathbf{n}_e} v \, ds \quad \forall v \in V. \quad (11)$$

The proof of residual formula derived by integrating by parts on each  $T$ .

Resulting boundary terms are collected in the term  $R_J$ .

## Error bound

Assuming that  $a_\alpha(\cdot, \cdot)$  is coercive on  $H^1(\Omega)$ , and inserting  $v = e_h$  in (8), we see that

$$\frac{1}{c_0} |e_h|_{H^1(\Omega)}^2 \leq |a_\alpha(e_h, e_h)| = |R_h(e_h)|. \quad (12)$$

Therefore

$$\|e_h\|_{H^1(\Omega)} \leq c_0 \sup_{v \in H_0^1(\Omega)} \frac{|R_h(v)|}{\|v\|_{H^1(\Omega)}}. \quad (13)$$

The right-hand side of (13) is the  $H^{-1}(\Omega)$  norm of the residual.

This norm is in principle computable in terms of the data of the problem ( $f$  and  $\alpha$ ) and  $u_h$ .

But the typical approach is to estimate it using what is known as a Scott-Zhang [10] interpolant  $I_h$  which satisfies, for some constant  $c_0$ ,

$$\|v - I_h v\|_{L^2(T)} \leq c_0 h_T |v|_{H^1(\hat{T})} \quad (14)$$

for all  $T \in T_h$ , where  $\hat{T}$  denotes the union of elements that contact  $T$ , and

$$\|v - I_h v\|_{L^2(e)} \leq c_0 h_e^{1/2} |v|_{H^1(T_e)} \quad (15)$$

for all faces  $e$  in  $T_h$ , where  $T_e$  denotes the union of elements that share the face  $e$ , where  $h_e$  (resp.  $h_T$ ) is a measure of the size of  $e$  (resp.  $T$ ).

Dropping the subscript “ $e$ ” on the normal  $\mathbf{n}$  to  $e$ , we get

$$\begin{aligned} |R_h(v)| &= |R_h(v - I_h v)| \\ &= \left| \sum_T \int_T R_A(v - I_h v) dx \right. \\ &\quad \left. + \sum_e \int_e [\alpha \mathbf{n} \cdot \nabla u_h]_{\mathbf{n}} (v - I_h v) ds \right| \\ &\leq \sum_T \|R_A\|_{L^2(T)} \|v - I_h v\|_{L^2(T)} \\ &\quad + \sum_e \|[\alpha \mathbf{n} \cdot \nabla u_h]_{\mathbf{n}}\|_{L^2(e)} \|v - I_h v\|_{L^2(e)}. \end{aligned}$$

Thus

$$\begin{aligned} |R_h(v)| &\leq \sum_T \|R_A\|_{L^2(T)} c_0 h_T |v|_{H^1(\hat{T})} \\ &\quad + \sum_e \| [\alpha \mathbf{n} \cdot \nabla u_h]_{\mathbf{n}} \|_{L^2(e)} c_0 h_e^{1/2} |v|_{H^1(\hat{T}_e)} \\ &\leq c' \left( \sum_T \|R_A\|_{L^2(T)}^2 h_T^2 \right. \\ &\quad \left. + \sum_e \| [\alpha \mathbf{n} \cdot \nabla u_h]_{\mathbf{n}} \|_{L^2(e)}^2 h_e \right)^{1/2} |v|_{H^1(\Omega)}, \end{aligned} \tag{16}$$

where  $c' = C c_0$  for some constant  $C$  that depends only on the maximum number of elements in  $\hat{T}$  for each  $T$ .

In view of (16), the **local error indicator**  $\mathcal{E}_e$  is defined by

$$\begin{aligned}\mathcal{E}_e(u_h)^2 &:= \sum_{T \subset T_e} h_T^2 \|f + \nabla \cdot (\alpha \nabla u_h)\|_{L^2(T)}^2 \\ &\quad + h_e \| [\alpha \mathbf{n} \cdot \nabla u_h]_{\mathbf{n}} \|_{L^2(e)}^2.\end{aligned}\tag{17}$$

The previous inequalities can be summarized as

$$|R_h(v)| \leq c' \left( \sum_e \mathcal{E}_e(u_h)^2 \right)^{1/2} |v|_{H^1(\Omega)},\tag{18}$$

which in view of (13) implies that

$$|e_h|_{H^1(\Omega)} \leq c' c_0 \left( \sum_e \mathcal{E}_e(u_h)^2 \right)^{1/2},\tag{19}$$

where  $c'$  is a constant only related to interpolation error.

## Local error estimates and refinement

In the previous slide, an upper bound for the global error  $|u - u_h|_{H^1(\Omega)}$  was given in terms of locally defined error estimators (17).

If the data  $f$  and  $\alpha$  are themselves piecewise polynomials of some degree, there is a lower bound for the local error [4, Section 9.3]

$$|e_h|_{H^1(T_e)} \geq c \mathcal{E}_e(u_h) \quad (20)$$

where  $c > 0$  depends only on the non-degeneracy constant for  $T_h$ .

## Local error estimates and refinement

One corollary of (20) is reverse inequality to (19),

$$|e_h|_{H^1(\Omega)} \geq \frac{c}{\sqrt{2}} \left( \sum_{e \in T_h} \mathcal{E}_e(u_h)^2 \right)^{1/2}.$$

A reverse inequality to (20) (a local *upper* bound) is not true in general.

However, the local lower bound (20) suggests the philosophy that

the mesh should be refined wherever

the local error indicator  $\mathcal{E}_e(u_h)$  is big.

Unfortunately, ....

where indicator is small

error not necessarily small.

Distant effects may pollute the error and

make error large even if

error indicator  $\mathcal{E}_e(u_h)$  is small nearby.

It is possible to have error estimators for other norms.

For example, the pointwise error  $u - u_h$  at  $\mathbf{x}$  can be represented using the Green's function

$$\begin{aligned}(u - u_h)(\mathbf{x}) &= a_\alpha(u - u_h, G^{\mathbf{x}}) = a_\alpha(u - u_h, G^{\mathbf{x}} - v) \\ &= R_h(G^{\mathbf{x}} - v) \quad \forall v \in V_h.\end{aligned}\tag{21}$$

Thus choosing  $v$  as the Scott-Zhang interpolant of  $G^{\mathbf{x}}$  [5, page 719] leads to an error indicator of the form

$$\begin{aligned}\mathcal{E}^\infty(u_h) &= \max_{T \in T_h} \left( h_T^2 \|f + \nabla \cdot (\alpha \nabla u_h)\|_{L^\infty(T)} \right. \\ &\quad \left. + h_e \| [\alpha \mathbf{n} \cdot \nabla u_h]_{\mathbf{n}} \|_{L^\infty(e)} \right).\end{aligned}\tag{22}$$

It can be proved [5] that there is a constant  $C$  such that

$$\|u - u_h\|_{L^\infty(\Omega)} \leq C\mathcal{E}^\infty(u_h).$$

The error estimators in [5] apply as well to nonlinear problems and to singular perturbation problems.

An extension to anisotropic meshes is given in [6] for two-dimensional problems and piecewise linear approximation.

## Other goals

Instead of attempting to estimate norms of the error, we can estimate linear functionals of the error.

For example, the quantity of interest ( $C_6$ ) in the van der Waals problem is an integral.

The strategy of **goal oriented error estimation** [8] (a.k.a. **dual weighted residual method** [3]) is to solve a adjoint problem to find  $z \in V$  such that

$$a^*(z, v) = \mathcal{M}(v) \quad \forall v \in V, \quad (23)$$

where  $\mathcal{M}$  is the linear functional to be optimized.

## Form adjoint

Here, the adjoint form  $a^*(\cdot, \cdot)$  is defined for any bilinear form  $a(\cdot, \cdot)$  via

$$a^*(v, w) = a(w, v) \quad \forall v, w \in V. \quad (24)$$

The concept of adjoint form can also be extended [8] to the case where  $a(\cdot, \cdot)$  is defined on a pair of spaces  $V \times W$  instead of  $V \times V$  as is the usual case considered so far.

It is also possible to extend the theory to allow the goal functional  $\mathcal{M}$  to be nonlinear.

It works!

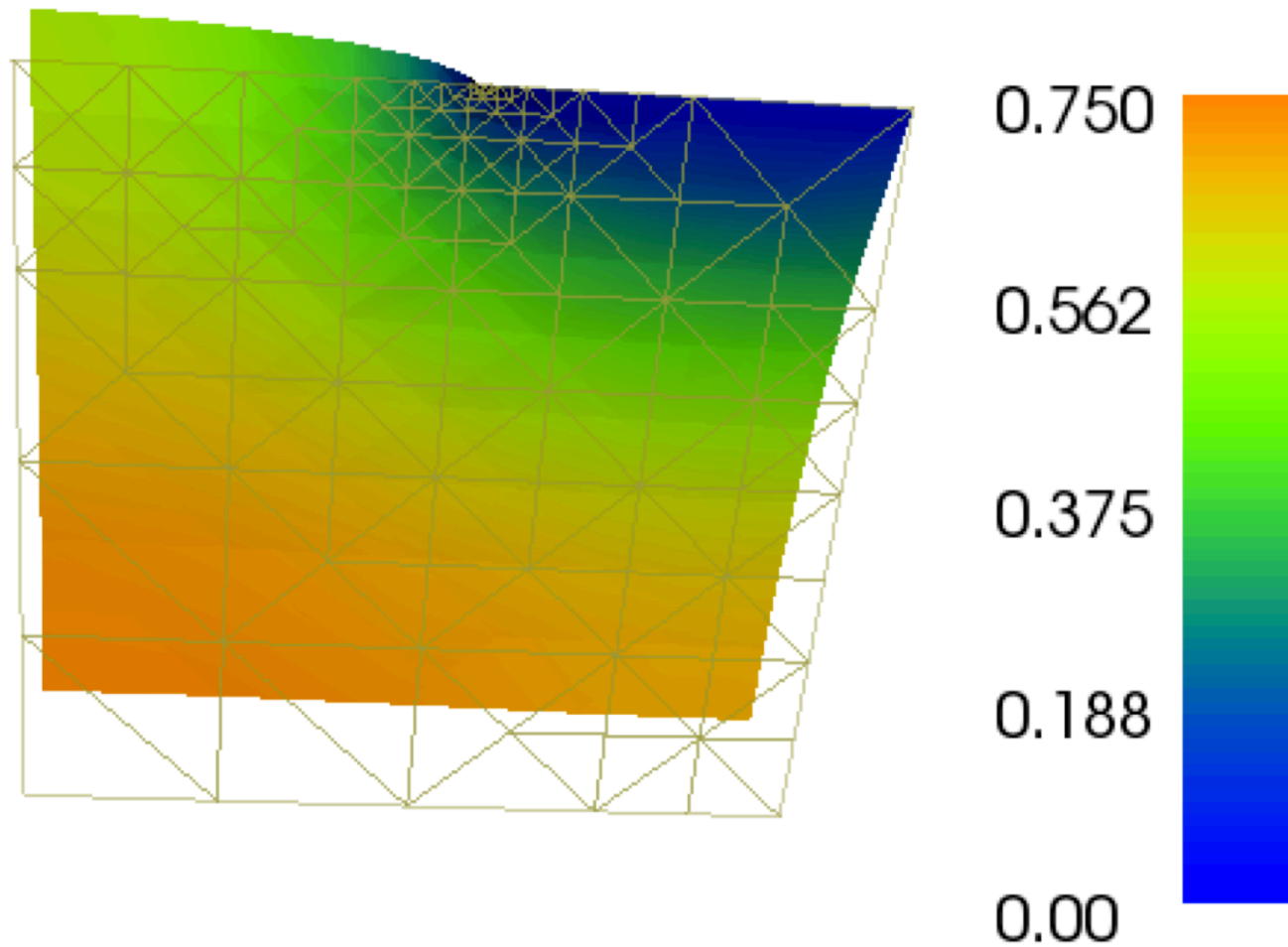


Figure 2: Adaptivity applied to the slit problem using piecewise linears and an initial mesh of size 4 with a goal  $\mathcal{M}(u) = \int_{\Omega} u^2 dx$ . The initial, unrefined mesh is apparent in the lower-left corner of the domain.

# The variational code

The variational formulation translates to code:

```
mytol=float(sys.argv[4])

.....

# Define boundary condition
u0 = Constant(0.0)
bc = DirichletBC(V, u0, boundary)

# Define variational problem
u = Function(V)
v = TestFunction(V)
f = Expression("1.0")
J = u*u*dx
F = (inner(grad(u), grad(v)))*dx - f*v*dx

# Compute solution
solve(F == 0, u, bc, tol=mytol, M=J)
```

## More about the adjoint form

If  $a(\cdot, \cdot)$  is symmetric, then  $a^*(\cdot, \cdot)$  is the same as  $a(\cdot, \cdot)$ . But it is different for the diffusion-advection form  $a_\beta(\cdot, \cdot)$ .

$$a_\beta(v, w) = \int_{\Omega} \nabla v(\mathbf{x}) \cdot \nabla w(\mathbf{x}) + (\beta(\mathbf{x}) \cdot \nabla v(\mathbf{x})) w(\mathbf{x}) d\mathbf{x}.$$

We see that, if  $\nabla \cdot \beta = 0$  and Dirichlet conditions are imposed on the boundary wherever  $\beta \cdot \mathbf{n} \neq 0$ , then

$$\begin{aligned} a_\beta^*(v, w) &= a_\beta(w, v) \\ &= \int_{\Omega} \nabla v(\mathbf{x}) \cdot \nabla w(\mathbf{x}) - (\beta(\mathbf{x}) \cdot \nabla v(\mathbf{x})) w(\mathbf{x}) d\mathbf{x} \quad (25) \\ &= a_{-\beta}(v, w) \quad \forall v, w \in V. \end{aligned}$$

## Using the adjoint form

Suppose as usual that  $u \in V$  satisfies  $a(u, v) = F(v)$  for all  $v \in V$ , that  $u_h \in V_h$  satisfies  $a(u_h, v) = F(v)$  for all  $v \in V_h$ , and that  $V_h \subset V$ .

Then  $a(u - u_h, v) = 0$  for all  $v \in V_h$ , and

$$\begin{aligned}\mathcal{M}(u) - \mathcal{M}(u_h) &= \mathcal{M}(u - u_h) = a^*(z, u - u_h) \\ &= a(u - u_h, z) \\ &= a(u - u_h, z - v) \\ &= R_h(z - v) \quad \forall v \in V_h.\end{aligned}\tag{26}$$

Analogy with (21): instead of Green's function  $G^x$

we have  $z$ .

## Other goals

Difficulty: do not know  $z$ , and need to compute it.

If we use same approximation space  $V_h$  to compute  $z_h$ , then we get a false impression (take  $v = z_h$  in (26)).

Need to have higher-order approximation of  $z$  than would normally be provided via  $V_h$ .

Different approaches to achieving this have been studied [3], including simply approximating via a globally higher-order method.

## What `dolfin` does

What is done in `dolfin` [8] (see also [3]) is to first compute  $z_h$ , then interpolate it on patches around a given element using a higher-degree approximation, using the interpolant as an approximation to  $z$ .

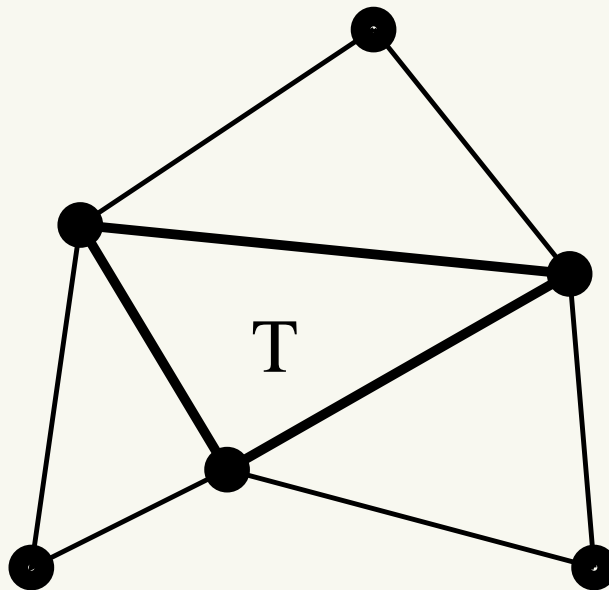


Figure 3: Nearby elements are used to construct a higher-order approximation to  $z$ .

## What magic `dolphin` does

Approach is effective and inexpensive, but ....  
if this gives higher-order accuracy, why not use it?

There may be singularities in  $z$  that make its approximation poor.

Duality between estimating the accuracy of  $u_h$  and the approximation of  $z$  [3] can address this.

But there is a certain amount of art in goal-based error estimation that cannot be fully justified rigorously.

## What dolfin does

In any case, the approach works as indicated in Figure 2, where the slit problem has been revisited using piecewise linears on an initial mesh of size 4 with a goal  $\mathcal{M}(u) = \int_{\Omega} u^2 d\mathbf{x}$ .

The initial, unrefined mesh is apparent in the lower-left corner of the domain.

## An example

Suppose that  $a(\cdot, \cdot)$  is symmetric, so that  $a^*(\cdot, \cdot) = a(\cdot, \cdot)$ , and that  $\mathcal{M}(v) = F(v)$ .

Then  $z = u$ .

Such a situation occurs in van der Waals problem, and we suggest it be explored further as an exercise.

## Boundary layers

Mesh refinement motivated so far by point singularities.

However, theoretical foundations of error estimation are insensitive to nature of singularities.

Boundary layers have singularities near large segments (or all of) domain boundary.

Recall the problem

$$-\epsilon \Delta u + u = 1 \text{ in } \Omega, \quad u = 0 \text{ on } \partial\Omega.$$

Results depicted in Figure 4 for  $\epsilon = 0.001$ .

## Boundary layer adapted mesh

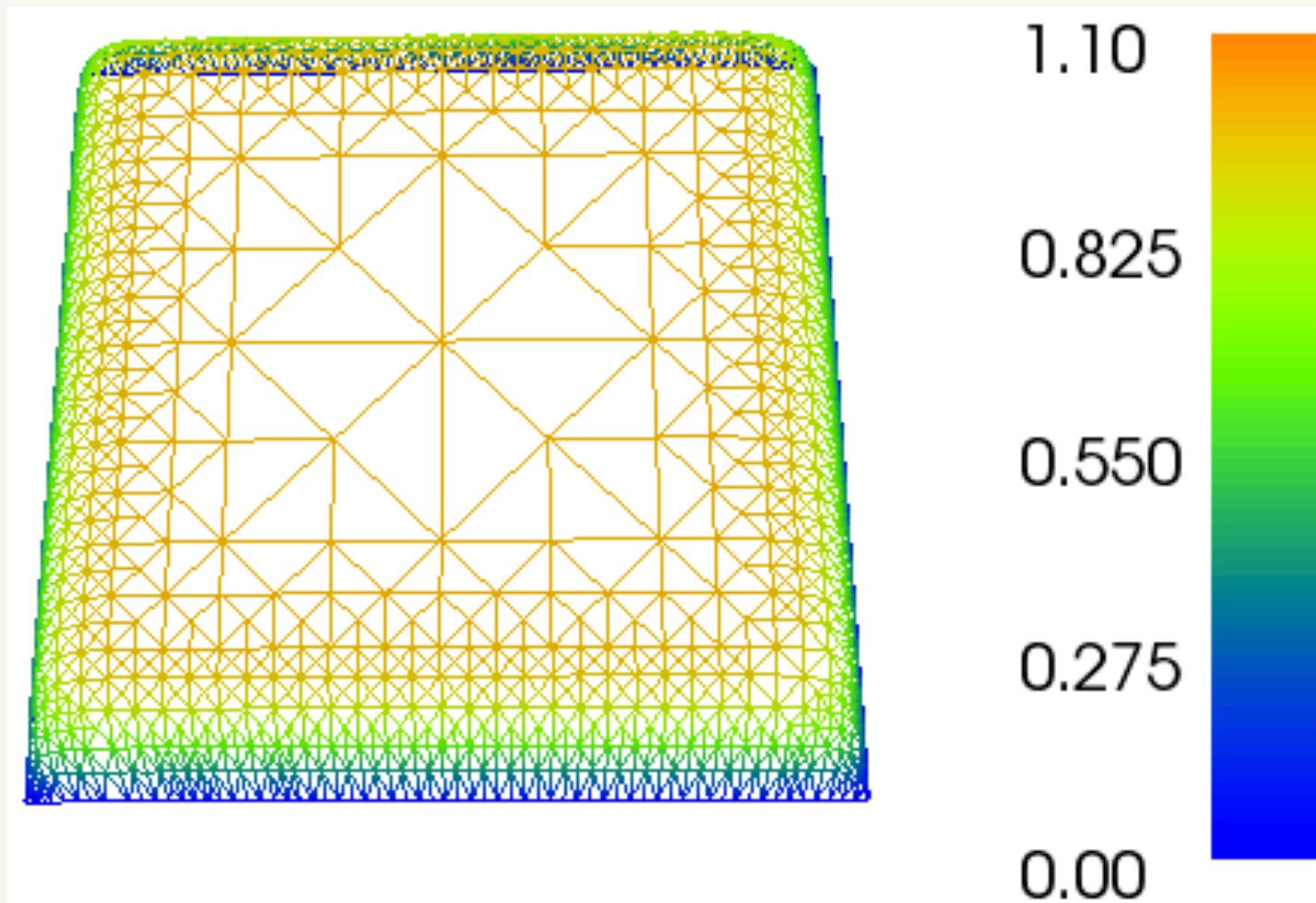


Figure 4: Adaptivity using piecewise linears and an initial mesh of size 2 with a goal  $\mathcal{M}(u) = \int_{\Omega} u^2 dx$ . Coarsest mesh elements apparent in middle of the domain, and refinement is made all around the boundary, with special concentration at four corners of square.

## Model problem

We have chosen a representation where we plot the mesh on the contours of the solution.

It appears that the automated techniques have accurately determined where mesh refinement was needed.

The computations were done with piecewise linears and a goal  $\mathcal{M}(u) = \int_{\Omega} u^2 d\mathbf{x}$ .

The remnants of the initial mesh are visible in the middle of the domain.

# References

- [1] Mark Ainsworth and J. Tinsley Oden. A posteriori error estimation in finite element analysis. *Computer Methods in Applied Mechanics and Engineering*, 142(1):1–88, 1997.
- [2] Ivo Babuška and Werner C. Rheinboldt. A-posteriori error estimates for the finite element method. *International Journal for Numerical Methods in Engineering*, 12(10):1597–1615, 1978.
- [3] Roland Becker and Rolf Rannacher. An optimal control approach to a posteriori error estimation in finite element methods. *Acta Numerica 2001*, 10:1–102, 2001.
- [4] Susanne C. Brenner and L. Ridgway Scott. *The Mathematical Theory of Finite Element Methods*. Springer-Verlag, third edition, 2008.
- [5] Alan Demlow and Natalia Kopteva. Maximum-norm a posteriori error estimates for singularly perturbed elliptic reaction-diffusion problems. *Numerische Mathematik*, 133:707742, 2016.
- [6] Natalia Kopteva. Maximum-norm a posteriori error estimates for singularly perturbed reaction-diffusion problems on anisotropic meshes. *SIAM Journal on Numerical Analysis*, 53(6):2519–2544, 2015.
- [7] Ekkehard Ramm, E. Rank, R. Rannacher, K. Schweizerhof, E. Stein, W. Wendland, G. Wittum, Peter Wriggers, and Walter Wunderlich. *Error-controlled adaptive finite elements in solid mechanics*. John Wiley & Sons, 2003.
- [8] Marie E. Rognes and Anders Logg. Automated goal-oriented error control i: Stationary variational problems. *SIAM Journal on Scientific Computing*, 35(3):C173–C193, 2013.
- [9] Rüdiger Verfürth. *A posteriori error estimation techniques for finite element methods*. Oxford University Press, 2013.
- [10] S. Zhang and L. R. Scott. Finite element interpolation of non-smooth functions satisfying boundary conditions. *Math. Comp.*, 54:483–493, 1990.